

## Senescing human cells and ageing mice accumulate DNA lesions with unrepairable double-strand breaks

Olga A. Sedelnikova<sup>1</sup>, Izumi Horikawa<sup>2</sup>, Drazen B. Zimonjic<sup>3</sup>, Nicholas C. Popescu<sup>3</sup>, William M. Bonner<sup>1</sup> and J. Carl Barrett<sup>2</sup>

**Humans and animals undergo ageing, and although their primary cells undergo cellular senescence in culture, the relationship between these two processes is unclear<sup>1,2</sup>. Here we show that  $\gamma$ -H2AX foci ( $\gamma$ -foci), which reveal DNA double-strand breaks (DSBs)<sup>3,4</sup>, accumulate in senescing human cell cultures and in ageing mice. They colocalize with DSB repair factors, but not significantly with telomeres. These cryptogenic  $\gamma$ -foci remain after repair of radiation-induced  $\gamma$ -foci, suggesting that they may represent DNA lesions with unrepairable DSBs. Thus, we conclude that accumulation of unrepairable DSBs may have a causal role in mammalian ageing.**

Three normal human cell strains and five mouse organs were examined throughout their lifespans for the incidence of  $\gamma$ -foci (Fig. 1a–c). In normal human fibroblasts (Fig. 1a, NHF) approaching senescence, both the incidence of  $\gamma$ -foci and the fraction of senescence-associated  $\beta$ -galactosidase-positive cells (SA- $\beta$ -gal)<sup>5</sup> increased with passage, accompanied by a progressive decrease in the fraction of foci-free cells. Similar relationships were identified in two other normal human cell strains: WI38 fibroblasts and PrEC prostate epithelial cells (Fig. 1f; WI38 and PrEC, black and hatched bars). Thus, the increase of  $\gamma$ -foci (from 0.2–0.3 foci per cell in early-passage cultures to 2.2–4.1 foci per cell in senescent cultures) may be a general process in human cell strains, including those of epithelial and fibroblastic origin.

Some exogenous agents induce premature senescence in normal human cells<sup>6,7</sup>. Exposure of NHF cultures at early passage (Passage 17 (P17)) to increasing concentrations of bleomycin (Fig. 1b) or  $H_2O_2$  (not shown) resulted in increased incidences of SA- $\beta$ -gal-positive cells and  $\gamma$ -foci when assessed after 5 days.  $H_2O_2$ -treated (100  $\mu$ M for 2 h) NHF cultures with 48% SA- $\beta$ -gal-positive cells contained  $2.0 \pm 0.5$   $\gamma$ -foci per cell and 30% foci-free cells, similarly to bleomycin-treated (1 mU ml<sup>-1</sup>) cultures and untreated P30 NHF cells. The similar frequency of  $\gamma$ -foci in cultures exhibiting similar senescent criteria, whether from continued culturing or from chemical exposure, suggests that these  $\gamma$ -foci may have a common origin and a causal role in senescence.

Cells taken from five different tissues of older mice exhibited increased numbers of  $\gamma$ -foci and lower numbers of foci-free cells (Fig. 1c) with values similar to those found for senescent human cells in culture. These changes occurred in both murine somatic and germ tissues; the imaged testes cells are late-pachytene primary spermatocytes, which contain large  $\gamma$ -H2AX positive sex-bodies (arrowheads)<sup>8</sup>. Thus, the accumulation of  $\gamma$ -foci is a common process in mammalian ageing *in vivo* and in culture.

Telomere shortening is one mechanism of cellular senescence in human cultured cells<sup>1,9</sup>. We assessed the extent of colocalization between  $\gamma$ -foci and telomeres in NHF cells. Twenty percent of the  $\gamma$ -H2AX signals coincided with telomere signals in replicatively senescent cultures, 11% in the prematurely senescent cultures, and occasionally in early-passage cultures (Fig. 1d, left three images). Although these results may suggest that some of the  $\gamma$ -foci are localized at or near telomeres in senescent cells, as shown in a recent report<sup>10</sup>, the frequencies of colocalization are close to stochastic values (15% and 9% for the replicatively and prematurely senescent cultures, respectively). There is also the possibility that very short telomeres were not detected in this experiment. However, this data and data from aged mouse tissues, in which only the occasional  $\gamma$ -focus overlapped with a telomere (Fig. 1d, right two images), coupled with the finding that ageing in mice does not involve gross reductions in telomere length<sup>7</sup>, strongly support a non-telomeric origin for the majority of cryptogenic  $\gamma$ -foci.

Further support for this conclusion comes from the fact that NHF cells ectopically expressing telomerase reverse transcriptase (TERT) contain elongated telomeres. These cells contain  $2.7 \pm 0.4$   $\gamma$ -foci per cell (Fig. 1f, immortal, black bar), similarly to senescent NHF cells and several human cancer cell lines (unpublished observations). Other studies have identified TERT-positive BJ cells containing large  $\gamma$ -foci that do not colocalize with telomeres<sup>11</sup>. When defective telomeres were artificially generated through expression of a dominant-negative mutant of the telomere-binding factor TRF2 (refs 10, 11), more  $\gamma$ -foci appeared that colocalized with telomeres. These foci were uniformly small and easily distinguished from the large  $\gamma$ -foci. The distinct morphology of the two types of  $\gamma$ -foci substantiates our evidence that shortening of the telomeres contributes only partially to the accumulation of the cryptogenic  $\gamma$ -foci in physiologically senescing human cells.

DSB-repair factors were identified in the cryptogenic  $\gamma$ -foci. Almost complete colocalization between the  $\gamma$ -foci and repair proteins 53bp1, Mre11, Rad50 and Nbs1 was observed in P17 NHFs (data not presented), P32 NHFs (Fig. 1e; P32 NHF control) and mice (see Supplementary Information, Fig. S1, mouse brain at 20 months; other tissues gave similar results (data not shown)), indicating that the  $\gamma$ -foci contain DSBs and further substantiating a common origin for the cryptogenic  $\gamma$ -foci observed in these two experimental systems.

<sup>1</sup>Laboratory of Molecular Pharmacology, <sup>2</sup>Laboratory of Biosystems and Cancer and <sup>3</sup>Laboratory of Experimental Carcinogenesis, Center for Cancer Research, National Cancer Institute, National Institutes of Health, Bethesda, MD, 20892, USA.

<sup>3</sup>Correspondence should be addressed to W.M.B. (e-mail: bonnerw@mail.nih.gov)

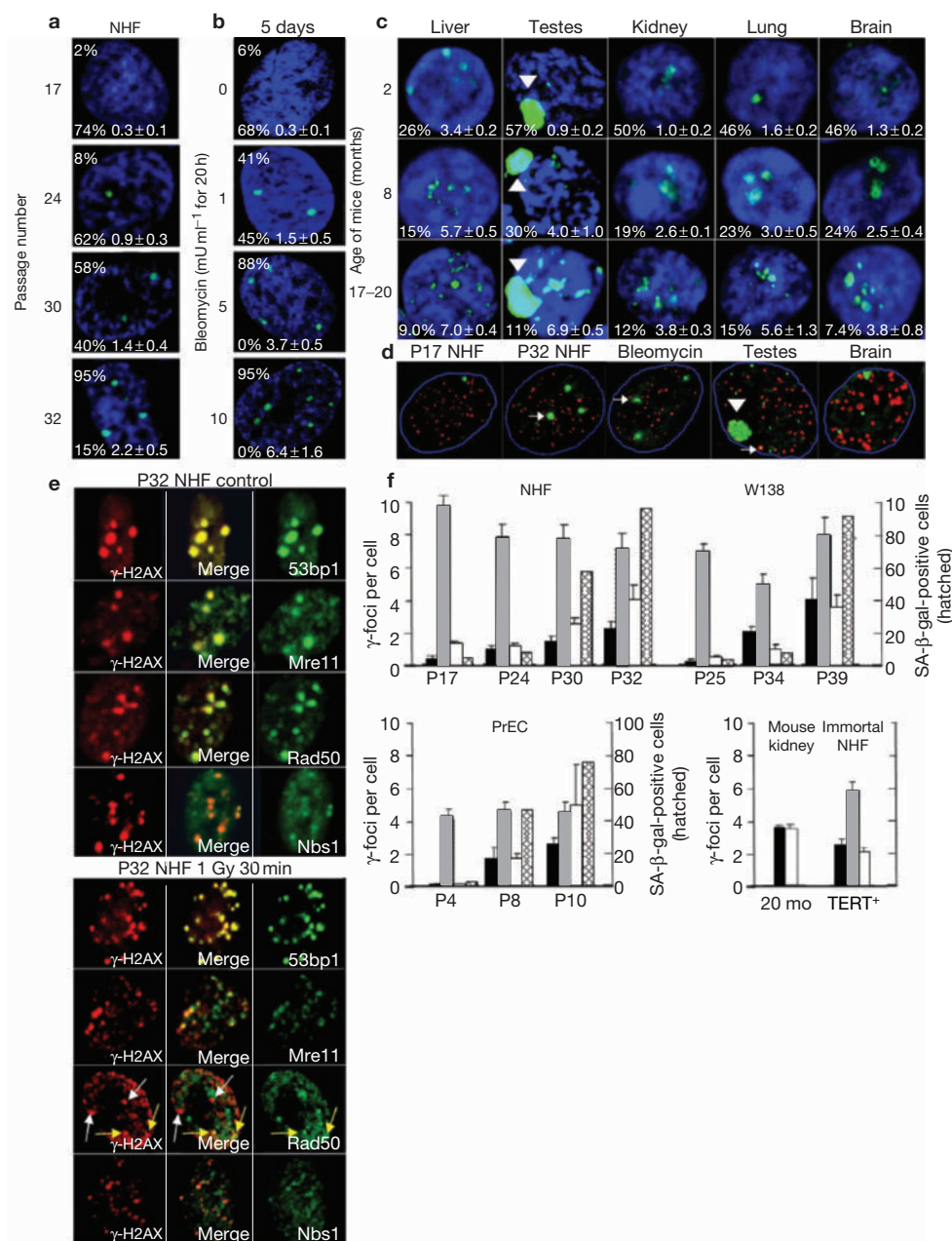


**Figure 1** Accumulation of  $\gamma$ -foci during senescence in culture and in ageing mice. **(a)** NHF cultures stained with anti- $\gamma$ -H2AX. Blue, propidium iodide; green,  $\gamma$ -H2AX. Each image represents a projection of all optical sections through a typical cell. The number of  $\gamma$ -foci per cell is shown in the lower right corner (average  $\pm$  standard error), the percentage of foci-free cells is shown in the lower left corner, and the percentage of SA- $\beta$ -gal-positive cells in the culture is shown in the upper left corner. **(b)** P17 NHF cultures exposed to bleomycin. Labelling is the same format as in **a**. **(c)**  $\gamma$ -foci in mice. Labelling is the same format as in **a**, except that there is no SA- $\beta$ -gal

data. **(d)** Telomeres and  $\gamma$ -foci (colocalization is marked by arrows). From left to right: typical cells from P17 and P32 NHF cultures, bleomycin-treated cultures, a mouse primary spermatocyte and a brain cell. Green,  $\gamma$ -H2AX; red, PNA probe. Arrowheads in **c** and **d** denote sex bodies. **(e)** DNA DSB repair proteins and  $\gamma$ -H2AX foci in P32 NHF cultures. Merged images are also shown. Yellow arrows,  $\gamma$ -foci overlapping Rad50; white arrows,  $\gamma$ -foci lacking Rad50. **(f)** Permanence of cryptogenic  $\gamma$ -foci. Black bars, non-irradiated cells; shaded bars, 30 min after irradiation; white bars, 24 h after irradiation; hatched bars, fraction of SA- $\beta$ -gal-positive cells.

Similarly to un-irradiated cultures, cultures at 16 h post-irradiation (see Supplementary Information, Fig. S1; P32 NHF, 1 Gy, 16 h) exhibited almost complete colocalization between  $\gamma$ -foci and DSB repair proteins. Results were more variable at 30 min post-irradiation (Fig. 1e; P32 NHF, 1 Gy, 30 min), possibly as a result of the differing accumulation rates of the different repair protein species at nascent

$\gamma$ -foci<sup>12, 13</sup>. Several  $\gamma$ -foci seemed to contain Rad50 (Fig. 1e, yellow arrows) at 30 min post-irradiation, whereas others seemed to lack Rad50 (Fig. 1e, white arrows). Thus, repair protein content may distinguish cryptogenic  $\gamma$ -foci from nascent  $\gamma$ -foci. This observation supports the model of two types of  $\gamma$ -foci: transient (where successful DSB rejoining occurs) and persistent (containing unreparable DSBs).

A prediction from this model is that the incidence of total cryptogenic  $\gamma$ -foci should return to the respective pre-irradiation incidence after DSB repair is complete. We examined the numbers of  $\gamma$ -foci in human cells 30 min after irradiation (Fig. 1f, shaded bars) and 24 h later, when radiation-induced foci were repaired (Fig. 1f, white bars). In three human cell strains, TERT-positive NHF cells and mouse tissues, the incidences of  $\gamma$ -foci at 24 h returned to values similar to those detected before irradiation. Thus, it is likely that the cryptogenic  $\gamma$ -foci are persistent and mark unreparable lesions.

These findings indicate that during cellular senescence or organismal ageing, mammalian cells accumulate persistent DNA lesions that contain unreparable DSBs. This accumulation occurs in germ, as well as somatic, cells. The induction of persistent  $\gamma$ -foci during exposure of cells to exogenous agents in numbers similar to those found in comparable replicative senescence supports a concept that accumulating unreparable DSB-containing lesions may have a causal role in ageing. Thus, this study establishes the physiological importance of unreparable DSB-containing lesions in cellular and organismal ageing, and raises the possibility that diverse factors that affect ageing may all function ultimately through the accumulation of persistent DNA lesions containing unreparable DSBs.

## METHODS

**Cell cultures.** NHFs derived from foreskin were a gift from J. Boyer (University of North Carolina, NC). WI38 human fibroblasts from Coriell Cell Repositories (Camden, NJ); human prostate epithelial cells (PrEC) were purchased from Clonetics (San Diego, CA). TERT-positive NHFs were previously described<sup>14</sup>. Cultures were maintained according to standard protocols. For immunofluorescence microscopy, cells were seeded on Labtek II four-well glass slides (Nalge Nunc International, Naperville, IL) at a density of  $2 \times 10^5$  cells per well. SA- $\beta$ -gal activity was detected as previously described<sup>5</sup>. Cells were either irradiated (0.6 Gy) in a Mark I  $\gamma$ -irradiator and fixed after a 30-min incubation at 37 °C, or treated with different concentrations of bleomycin sulfate or H<sub>2</sub>O<sub>2</sub> (Sigma, St. Louis, MO) for 20 or 2 h, respectively. Concentrations of bleomycin (1–10 mU ml<sup>-1</sup>) or H<sub>2</sub>O<sub>2</sub> (100–200  $\mu$ M) were calibrated to induce premature senescence. Cultures were incubated for 5 days before processing to allow repairable  $\gamma$ -foci to be resolved and senescent phenotypes to be expressed.

**Laser-scanning confocal microscopy (LSCM).** Cultures on Labtek II slides were processed for immunofluorescence microscopy as previously described<sup>3</sup>. For double labelling, the  $\gamma$ -H2AX primary antibody was from rabbit or mouse (Upstate BioTech, Lake Placid, NY) depending on the origin of the other antibodies; either 53bp1, Mre11, Rad50 or Nbs1. Antibodies were: anti-53bp1, a generous gift from J. Chen (Department of Oncology, Mayo Clinic and Foundation), anti-Nbs1, a kind gift from A. Nussenzweig (Experimental Immunology Branch, Center for Cancer Research, National Cancer Institute, National Institutes of Health), anti-Mre11 and anti-Rad50 (Novus Biologicals,

Littleton, CO). LSCM was performed with a Nikon PCM 2000 (Nikon, Augusta, GA). Foci were counted by eye in at least 35 cells. Five independent determinations of the P17 NHF control (from replicative senescence, bleomycin treatment and H<sub>2</sub>O<sub>2</sub> treatment) yielded values of  $0.1\text{--}0.3 \pm 0.1$  foci per cell. For telomeres, samples already immunostained for  $\gamma$ -H2AX were treated with 50 mM ethylene glycol-*bis* (succinic acid *N*-hydroxy-succinimide ester; E-3257; Sigma, St. Louis, MO) for 30 min at 37 °C, incubated in RNase (100  $\mu$ g ml<sup>-1</sup>), washed in TBS, ethanol-dehydrated at -20 °C, air-dried, denatured in NaOH (pH 12.45)/ethanol, rinsed, dehydrated again, dried, hybridized with heat-denatured telomere peptide nucleic acid (PNA) Cy3-conjugated probe (DAKO A/S, Denmark) for 1 h at 37 °C, washed with 70% formamide/PBS at pH 7.4, dehydrated at -20 °C, stained in DAPI/PBS and mounted in antifade for confocal microscopy detection (method modified from ref. 15). The stochastic frequencies of the extent of colocalization between telomeres and  $\gamma$ -H2AX were calculated on the basis of relative areas of the foci and nuclear sections.

**Mouse tissues.** Male mice were obtained from the National Institute of Aging, Aged Rodent Colonies (Bethesda, MD; 2-, 8- and 20-month old C57BL/6 mice) or from the Experimental Immunology Branch, CCR, NCI (2- and 17-month old C57BL/6 mice). Organs were removed and touch-printed for analysis by immunofluorescence microscopy. At least 40 cells from each organ of five mice from each aging group were examined.

Supplementary Information is available on the Nature Cell Biology website.

## ACKNOWLEDGMENTS

We thank C. Redon, D. Pilch and T. Furuta for their thoughtful advice, and I. Kareva for her technical assistance.

## COMPETING FINANCIAL INTERESTS

The authors declare that they have no competing financial interests.

Received 3 November 2003; accepted 7 January 2004;

Published online at <http://www.nature.com/naturecellbiology>.

1. Hornsby, P. J. *J. Gerontol. A Biol. Sci. Med. Sci.* **57**, B251–B256 (2002).
2. Hanahan, D. & Weinberg, R. A. *Cell* **100**, 57–70 (2000).
3. Rogakou, E. P., Boon, C., Redon, C. & Bonner, W. M. *J. Cell Biol.* **146**, 905–915 (1999).
4. Sedelnikova, O. A., Rogakou, E. P., Panutyn, I. G. & Bonner, W. M. *Rad. Res.* **158**, 486–492 (2002).
5. Dimri, G. P. *et al. J. Proc. Natl Acad. Sci. USA* **92**, 9363–9367 (1995).
6. Robles, S. J. & Adami, G. R. *Oncogene* **16**, 1113–1123 (1998).
7. Horikawa, I., Yawata, T. & Barrett, J. C. *J. Anti-Aging Medicine* **3**, 373–382 (2000).
8. Fernandez-Capetillo, O. *et al. Dev. Cell.* **4**, 497–508 (2003).
9. Hasty, P., Campisi, J., Hoeijmakers, J., van Steeg, H. & Vijg, J. *Science* **299**, 1355–1359 (2003).
10. d'Adda di Fagnana F. *et al. Nature* **426**, 194–198 (2003).
11. Takai, H., Smogorzewska, A. & de Lange, T. *Cur. Biol.* **13**, 1549–1556 (2003).
12. Celeste, A. *et al. Science* **296**, 922–927 (2002).
13. Paull, T. T., Rogakou, E. P., Yamazaki, V., Kirchgessner, C. U., Gellert, M. & Bonner, W. M. *Curr. Biol.* **10**, 886–895 (2000).
14. Horikawa, I. *et al. Mol. Biol. Cell.* **13**, 2585–2597 (2002).
15. Chen, H. T. *et al. Science* **290**, 1962–1964 (2000).

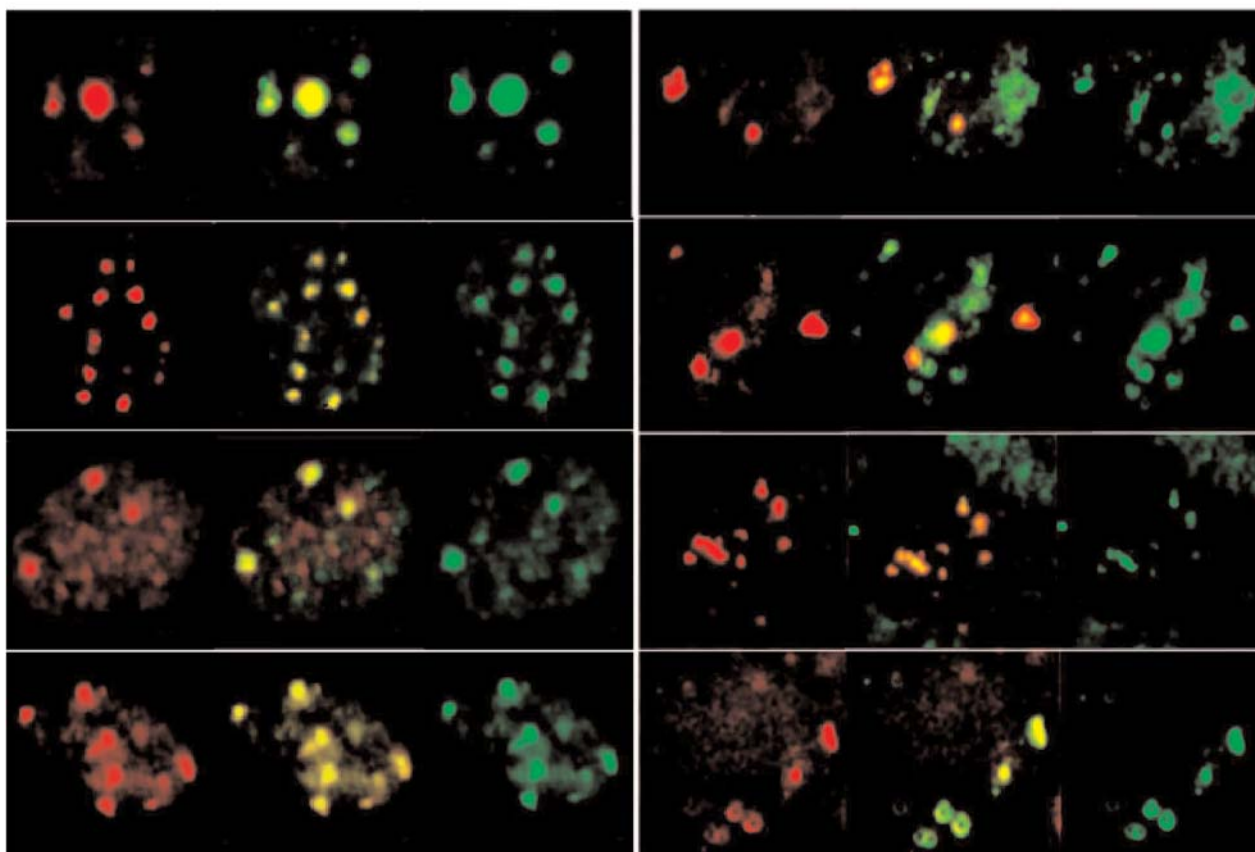


**Figure S1.** Colocalization of DNA DSB repair proteins with  $\gamma$ -H2AX foci in P32 NHF cultures taken 16 h after receiving 1 Gy and in brain cells from a 20 month-old mouse. The merged images are shown between the single-channel images.